



# UNIVERSITÀ DI PARMA

## ARCHIVIO DELLA RICERCA

University of Parma Research Repository

A mechanistic investigation on kokumi-active  $\gamma$ -Glutamyl tripeptides – A computational study to understand molecular basis of their activity and to identify novel potential kokumi-tasting sequences

This is the peer reviewed version of the following article:

*Original*

A mechanistic investigation on kokumi-active  $\gamma$ -Glutamyl tripeptides – A computational study to understand molecular basis of their activity and to identify novel potential kokumi-tasting sequences / Dellafiora, Luca; Magnaghi, Fabio; Galaverna, Gianni; Dall'Asta, Chiara. - In: FOOD RESEARCH INTERNATIONAL. - ISSN 0963-9969. - 162:(2022), p. 111932. [10.1016/j.foodres.2022.111932]

*Availability:*

This version is available at: 11381/2929473 since: 2024-10-03T15:38:20Z

*Publisher:*

*Published*

DOI:10.1016/j.foodres.2022.111932

*Terms of use:*

Anyone can freely access the full text of works made available as "Open Access". Works made available

*Publisher copyright*

note finali coverpage

(Article begins on next page)

# Food Research International

## A mechanistic investigation on kokumi-active $\gamma$ -Glutamyl tripeptides – a computational study to understand molecular basis of their activity and to identify novel potential kokumi-tasting sequences --Manuscript Draft--

<b>Manuscript Number:</b>	FOODRES-D-22-02095R2
<b>Article Type:</b>	Research Paper
<b>Keywords:</b>	$\gamma$ -glutamyl peptides; kokumi; Molecular modeling; taste receptors; calcium-sensing receptor
<b>Corresponding Author:</b>	Luca Dellafiora University of Parma ITALY
<b>First Author:</b>	Luca Dellafiora
<b>Order of Authors:</b>	Luca Dellafiora Fabio Magnaghi Gianni Galaverna Chiara Dall'Asta
<b>Abstract:</b>	<p>Kokumi is an important taste perception whose chemical basis still needs clarifications and for which the development of high-throughput tools of analysis is desirable. The activation of Calcium-sensing receptor (CaSR) was described as the molecular initiating event of kokumi perception allowing the use of molecular modelling to deepen its chemical basis and related mechanisms. This study focused on <math>\gamma</math>-Glutamyl tripeptides, computationally investigated mechanistic basis of their CaSR-activating properties and extended the comprehension of their structure-activity relationship. A library of 400 <math>\gamma</math>-Glutamyl tripeptides was also screened. <math>\gamma</math>-Glu-Pro-Ala and <math>\gamma</math>-Glu-Pro-Ser were identified for further dedicated investigations based on their promising CaSR-activating potential and their presence should be checked accordingly in food matrices to better profile the kokumi fingerprint. This work provided a meaningful tool for the top-down analysis of kokumi-active molecules that may support either the identification of kokumi molecules concealed in food or the rational design of kokumi-active molecules de novo .</p>
<b>Suggested Reviewers:</b>	Gianni Sagratini gianni.sagratini@unicam.it  Jeffrey L. Ram jeffram@wayne.edu  Jihan Kim jihan.kim@agresearch.co.nz  Moronaka Kuroda motonaka_kuroda@ajinomoto.com  Rene Lametsch rla@food.ku.dk

## Highlights

- Mechanistic and chemical basis of kokumi  $\gamma$ -Glutamyl tripeptides has been depicted
- The stabilization of the closed conformation of Calcium-sensing receptor was modeled
- Specific receptor movements were monitored to assess kokumi activity of molecules
- A virtual library of 400  $\gamma$ -Glutamyl tripeptides was screened
- $\gamma$ -Glu-Pro-Ala and  $\gamma$ -Glu-Pro-Ser were described as potential potent kokumi compounds

1 **A mechanistic investigation on kokumi-active  $\gamma$ -Glutamyl tripeptides – a computational**  
2 **study to understand molecular basis of their activity and to identify novel potential**  
3 **kokumi-tasting sequences**

4

5 Luca Dellafiora<sup>1\*</sup>, Fabio Magnaghi<sup>1</sup>, Gianni Galaverna<sup>1</sup>, Chiara Dall'Asta<sup>1</sup>

6 <sup>1</sup> Department of Food and Drug, University of Parma, Parco Area delle Scienze 27/A, 43124

7 Parma, Italy.

8

9 \* Correspondence to: Luca Dellafiora, Department of Food and Drug, University of Parma,

10 Parco Area delle Scienze 27/A, 43124 Parma, Italy. Phone: +39 0521 906070. Email:

11 [luca.dellafiora@unipr.it](mailto:luca.dellafiora@unipr.it)

12 **Abstract**

13 Kokumi is an important taste perception whose chemical basis still needs clarifications and  
14 for which the development of high-throughput tools of analysis is desirable. The activation  
15 of Calcium-sensing receptor (CaSR) was described as the basis of kokumi perception  
16 allowing the use of molecular modelling to deepen its chemical rationale and related  
17 mechanisms. This study focused on  $\gamma$ -Glutamyl tripeptides, computationally ~~investigated~~  
18 ~~mechanistic basis providing mechanistic insights on~~ of their CaSR-activating properties and  
19 extended the comprehension of their structure-activity relationship. A library of 400  $\gamma$ -  
20 Glutamyl tripeptides was also screened.  $\gamma$ -Glu-Pro-Ala and  $\gamma$ -Glu-Pro-Ser were identified for  
21 further dedicated investigations based on their promising CaSR-activating potential and  
22 their presence should be checked accordingly in food matrices to better profile the kokumi  
23 fingerprint. This work provided a meaningful tool for the top-down analysis of kokumi-active  
24 molecules that may support either the identification of kokumi molecules concealed in food  
25 or the rational design of kokumi-active molecules *de novo*.

26

27 *Keywords:*  $\gamma$ -glutamyl peptides, kokumi, molecular modeling, taste receptors, calcium-  
28 sensing receptor

## 29 1. Introduction

30 The term “kokumi” refers to as a complex taste sensation characterized by thickness,  
31 mouthfulness and continuity (Toelstede, Dunkel, & Hofmann, 2009; Toelstede & Hofmann,  
32 2008; Zhao, Schieber, & Ganzle, 2016). Such a sensation is important to determine taste,  
33 flavour, mouthfeel and aftertaste qualities of a wide variety of foods with critical  
34 implications for food acceptance and consequences on consumers behaviour and diet habits  
35 (Keast, Costanzo, & Hartley, 2021; Tang, Tan, Teo, & Forde, 2020). For this reason, the  
36 identification and characterization of kokumi-active molecules in food is an important piece  
37 of information, *inter alia*, to make connections between the chemistry of food and its  
38 perception and consumption. At the same time, the design of new kokumi-active molecules  
39 meant to be intentionally added in food can be important from a food design standpoint to  
40 endow designed food with desired flavour-related properties (e.g. (Ruijschop, Burseg,  
41 Lambers, & Overduin, 2009)). However, the kokumi-active fraction is hard to profile with  
42 precision in food due to experimental issues, and the *de novo* design of novel kokumi  
43 molecules is hampered by the uncomplete understanding of their structure-activity  
44 relationship.

45 From a mechanistic point of view, kokumi perception has been associated with the binding  
46 between kokumi-active molecules and the Calcium Sensing Receptor (CaSR), which results in  
47 its subsequent allosteric activation (Guha & Majumder, 2022). CaSR is a G-protein coupled  
48 receptor (GPCR) consisting in 1078 amino acids and expressed on the surface of diverse cell  
49 types. It has been under investigation since its discovery for its involvement in several  
50 pathologies (Huang, Zhao, Dong, & Hu, 2021; Sundararaman & van der Vorst, 2021).  
51 However, its expression was proved in the gustatory tissues of rats, further demonstrated in  
52 the taste buds in lingual epithelia, and the CaSR’s involvement was soundly proposed at the

53 basis of kokumi perception (Guha & Majumder, 2022; Maruyama, Yasuda, Kuroda, & Eto,  
54 2012; Ohsu et al., 2010). Specifically, the so called CaSR's Venus fly trap (VFT) domain has  
55 been described as the binding site of kokumi substances and its capability to close over  
56 ligands has been reported as the molecular initiating event underpinning CaSR activation  
57 and kokumi perception (Li, Zhang, & Lametsch, 2022; Wellendorph & Brauner-Osborne,  
58 2009).

59 Concerning the profiling of taste molecules in food, including kokumi-active compounds, the  
60 methods commonly used are still complex and time-consuming. They typically require  
61 composite multi-step experimental protocols based on the decomposition of a given matrix  
62 followed by the precise description of its taste-active chemical components (J. Kim et al.,  
63 2022; Vasilaki, Panagiotopoulou, Koupantsis, Katsanidis, & Mourtzinis). In line with the  
64 methods used to identify bioactive peptides of food origin, these methods can be defined  
65 "bottom-up" in the sense that they ideally require a comprehensive description of  
66 molecules in a certain food followed by their characterization in terms of taste activity  
67 (Schrader, 2018). Conversely, "top-down" approaches refer to techniques to create  
68 organized (bio)active structures either by etching down a bulk material or by engineering  
69 them into specific locations (Smith, Tejeda-Montes, Poch, & Mata, 2011). In the context of  
70 bioactive peptides of food origin, "top-down" approaches refer to food matrix-independent  
71 methods targeting the identification of bioactive sequences with specific features, the  
72 occurrence of which in food is searched after their bioactivity has been proved (Lammi et  
73 al., 2021). Similarly, taste-active molecules can be identified using "top-down" approaches  
74 defining their potential taste activity first, and then searching their presence in food  
75 matrices assessing their role in the overall food taste. In the context of kokumi-active  
76 molecules analysis, "top-down" approaches may ensure high-throughput investigations

77 providing ground either to better understand the chemistry underpinning the taste of  
78 specific foods *a posteriori*, or to support a knowledge-based design of taste molecules  
79 meant to be added in food.

80 In this context, computational analysis proved to efficiently support the characterization of  
81 taste molecules (Bo et al., 2022; J. Yang et al., 2021) with promising applications either for a  
82 bulk or precise discovery of novel taste-active compounds (Spaggiari, Di Pizio, & Cozzini,  
83 2020). In this context, the present work aimed at defining a 3D molecular modelling  
84 framework useful for a “top-down” identification of potent kokumi  $\gamma$ -Glutamyl tripeptides  
85 to: i) ~~decipher~~ get insights on the chemical and mechanistic basis of potent kokumi-active  $\gamma$ -  
86 Glutamyl tripeptides; and ii) to screen a combinatorial library of 400  $\gamma$ -Glutamyl tripeptides to  
87 identify novel and potentially potent kokumi-active sequences worthy of further dedicated  
88 investigations. The study focused on the class of  $\gamma$ -Glutamyl tripeptides as it includes potent  
89 kokumi-active compounds with glutathione (GSH,  $\gamma$ -Glu-Cys-Gly) and  $\gamma$ -Glu-Val-Gly among  
90 the most potent kokumi-active molecules described so far (Kuroda et al., 2013; Ohsu et al.,  
91 2010). The workflow described here focused on the molecular initiating event of kokumi  
92 taste and was based on docking simulations and molecular dynamics to study the  
93 interaction between  $\gamma$ -Glutamyl tripeptides and CasR, which has been recently described as  
94 the target taste receptor of kokumi molecules (Maruyama et al., 2012). Overall, this work  
95 presented a rational, useful and straightforward strategy either to better understand the 3D  
96 structure-activity relationship of kokumi-active  $\gamma$ -Glutamyl tripeptides or to identify new,  
97 potentially potent, and previously uncharacterized sequences for further analysis.

98

## 99 **2. Material and methods**

## 100 **2.1. Construction of $\gamma$ -Glutamyl tripeptides library, tryptophan and glycine residues**

101 The structures of  $\gamma$ -Glutamyl tripeptides analysed in this study were built using an in-house  
102 python script interfaced with PyMol (version 2.3.0; [www.pymol.org](http://www.pymol.org)). All possible duplets of  
103 the 20 proteogenic amino acids were generated, for a total of 400 combinations. These  
104 elements were symbolically represented by arrays of characters. The generated strings will  
105 be then divided into the representative characters of the single amino acid and added  
106 sequentially to the gamma carbon of the glutamate. The integrity of the carboxy-terminal  
107 was ensured adding an oxygen atom will be added to the carboxy terminal. The entire set of  
108 compounds generated was stored in the Protein Data Bank format (.pdb) first and then  
109 recursively converted in the Tripos Mol2 format (.mol2) for subsequent analysis using Open  
110 Babel (version 3.0.0) (O'Boyle et al., 2011) and setting the protonation state at pH 7 (i.e.,  
111 carboxy- and ammino-terminal set deprotonated and protonated, respectively). The  
112 consistency of binding geometries and bond and atom type assignment were visually  
113 inspected before further analysis.

114 The library included 400 different entries grouping all the possible combinations for  $\gamma$ -  
115 Glutamyl tripeptides with a  $\gamma$ -Glutamyl residues at the 1<sup>st</sup> position (Ammino terminus) and  
116 all the possible combinations including permutations of 20 proteinogenic amino acids at the  
117 2<sup>nd</sup> and 3<sup>rd</sup> position (Carboxy terminus).

118 The structure of L-tryptophan (L-Trp) and glycine (Gly) were retrieved from PubChem (S. Kim  
119 et al., 2021) in the 3D Structure Data File format (.sdf; CID 6305 and 750, respectively) and  
120 further converted in the .mol2 format as described above.

121

## 122 **2.2. Ligand-based virtual screening of $\gamma$ -Glutamyl tripeptides library**

123 The library of  $\gamma$ -Glutamyl tripeptides underwent a ligand-based virtual screening to sort  
124 entries according to their similarity to  $\gamma$ -Glu-Val-Gly, which is the most potent CaSR-activator  
125  $\gamma$ -Glutamyl tripeptide described *in vitro* so far (Ohsu et al., 2010). The ligand-based virtual  
126 screening was done using the LiSiCA (Ligand Similarity using Clique Algorithm) algorithm  
127 (Legnik et al., 2015). This algorithm provides a fast ligand-based virtual screening platform  
128 to quantify chemical similarities between a reference template (a strong kokumi  $\gamma$ -Glutamyl  
129 tripeptide in this case) and a database of target compounds. LiSiCA expresses similarities  
130 using the Tanimoto coefficient, a gold standard to quantify chemical analogies. LiSiCA's  
131 default parameters were used, with the exception of considering the 3D structures of  
132 ligands and setting the maximum allowed atom spatial distance for 3D product graph at 2, in  
133 agreement with a previous study (Lammi et al., 2021). This fast virtual screening procedure  
134 served to identify a short selection of sequences to carry forth to the slower and more  
135 demanding subsequent molecular modelling studies (see below).

136

### 137 **2.3. CaSR model construction**

138 The 3D model of human CaSR receptor was derived from the crystallographic structure  
139 recorded in the Protein Data Bank (<https://www.rcsb.org>; Berman et al., 2000) with PDB  
140 code 5FBK (chain A) (Zhang et al., 2016). This PDB record reported a high-resolution  
141 structure of the wild-type extracellular domain of human CaSR (residues 22-539), called  
142 venus flytrap (VFT) domain, which binds kokumi active molecules and is involved in the  
143 molecular initiating events of kokumi perception (Goralski & Ram, 2022; Mun et al., 2004).  
144 Such a structure was chosen based on its high higher resolution (2.10 Å) and more complete  
145 set of resolved coordinates compared to the others structure available at the time of

146 analysis (last database access 14<sup>th</sup> January 2022). However, it presented unresolved  
147 coordinates for residues 361-390, which were not available in any of the structures  
148 recorded in PDB at the time of analysis (last database access 14<sup>th</sup> January 2022). This portion  
149 consisted in a small peripheral domain the integrity of which was obtained combining data  
150 from homology modelling and expert structure editing. In more detail, the whole 3D  
151 structure of VTF domain (residues 22-539) was obtained first using trRosetta  
152 (<https://yanglab.nankai.edu.cn/trRosetta>) (J. Y. Yang et al., 2020) using the FASTA sequence  
153 of 5FBK structure, in agreement with a previous study (Louisse, Dorne, & Dellafiora, 2022).  
154 In more detail, trRosetta is an algorithm for a fast and accurate protein structure prediction  
155 that derive protein structures based on direct energy minimizations with a constrained  
156 optimization by Rosetta (Simons, Bonneau, Ruczinski, & Baker, 1999). The restraints include  
157 inter-residue distance and orientation distributions, predicted by a deep residual neural  
158 network. The model provided by trRosetta showed a high confidence with a TM score of 0.9  
159 (scores above 0.5 point to correct topological assignment, in agreement with previous  
160 studies (J. Y. Yang et al., 2020)). Such model was superimposed to the crystallographic  
161 structure and used to tailor the crystallographic structure by substituting the residues 338-  
162 402 ensuring the best backbone overlap between the model obtained from homology  
163 modelling and the crystallographic structure.

164

#### 165 **2.4. Docking studies**

166 The docking analysis aimed at providing a plausible binding architecture for L-Trp, Gly and  
167 the  $\gamma$ -Glutamyl tripeptides under investigation and was performed using the GOLD software  
168 (version 2021). The binding site has been defined within a 10-angstrom radius sphere

169 centred at the centroid of the substrate binding site of the VTF domain model with the xyz  
170 coordinates set in correspondence with the alpha-carbon of the crystallographic ligands of  
171 5FBK (Zhang et al., 2016). Docking protocol was set according to previous studies keeping  
172 ligands fully flexible (i.e. all the routable bonds were set free to rotate) and protein semi-  
173 flexible allowing polar hydrogens free to rotate (Dellafiora et al., 2017). As a minor  
174 modification, 10 poses for each ligand were generated and scored using the internal scoring  
175 function GOLDScore as it has been optimized for the prediction of ligand binding positions,  
176 according to the manufacturer declaration (<https://www.ccdc.cam.ac.uk>). Considering that  
177 the scoring assignment is proportional to the ligand-pocket fitting (the higher the score, the  
178 higher the match to the pocket physico-chemical properties), only the best scored pose for  
179 each docked ligand was considered for the analysis, in agreement with previous studies  
180 (Dellafiora et al., 2017). Also, the positioning of each ligand was facilitated using the  
181 “Similarity constraint” option choosing the crystallographic pose of 5FBK’s ligand as  
182 template and choosing to avoid the generation of docking poses when the constraint is  
183 physically impossible.

184 Moreover, GOLD uses a genetic algorithm that may introduce variability in the score  
185 assignment. Therefore, each ligand was run in triplicate to check the respective scoring  
186 fluctuations. Score assignment was found reliably stable for active compounds (further  
187 details are reported in the Results and Discussion section) with a maximum coefficient of  
188 variation below 0.9 % (scores are expressed as mean  $\pm$  standard deviation).

189 RMSD values between the calculated and crystallographic poses of L-Trp were calculated  
190 using the align command implemented in PyMol disallowing cycles correction and  
191 considering the all set of not-hydrogen atoms.

192

## 193 **2.5. Pharmacophoric analysis**

194 The pocket of VFT domain was defined using GetCleft (Gaudreault, Morency, &  
195 Najmanovich, 2015), while the respective pharmacophoric fingerprint was derived using the  
196 IsoMIF algorithm (Chartier & Najmanovich, 2015), as previously described (Lammi et al.,  
197 2021).

198

## 199 **2.6. Molecular dynamics**

200 Molecular dynamics aimed at studying the stability of VTF domain in complex with the  
201 various ligands over the time. They were performed using GROMACS (version 2019.4)  
202 (Abraham et al., 2015) with CHARMM27 all-atom force field parameters support (Best et al.,  
203 2012) for protein, L-Trp and Gly.  $\gamma$ -Glutamyl tripeptides have been processed and  
204 parameterized with CHARMM27 all-atom force field using the SwissParam tool  
205 (<http://www.swissparam.ch>) (Zoete, Cuendet, Grosdidier, & Michielin, 2011). Input  
206 structures were solvated with SPCE waters in a cubic periodic boundary condition, and  
207 counter ions ( $\text{Na}^+$  or  $\text{Cl}^-$ ) were added to neutralize the system. Prior to running simulations,  
208 each system was energetically minimized to avoid steric clashes and to correct improper  
209 geometries using the steepest descent algorithm with a maximum of 5,000 steps.  
210 Afterwards, all the systems underwent isothermal (300 K, coupling time 2 psec) and isobaric  
211 (1 bar, coupling time 2 psec) 100 psec simulations before running 25 nsec simulations (300 K  
212 with a coupling time of 0.1 psec and 1 bar with a coupling time of 2.0 psec).

213

## 214 **3. Results and Discussion**

215 Kokumi perception is a complex phenomenon, and its underpinning early mechanisms  
216 depend on the activation of CaSR. CaSR is a class C G protein-coupled receptor (GPCR)  
217 working as a homodimer with a large extracellular VFT domain, which is involved in the  
218 recognition of kokumi active molecules (Ling et al., 2021). The network of molecular  
219 mechanisms underpinning the activation of CaSR and the transduction of signal through the  
220 membrane is complex and still need clarifications. However, the capability of VFT domain to  
221 close over ligands has been described as the molecular initiating event underpinning CaSR  
222 activation and kokumi perception (Wellendorph & Brauner-Osborne, 2009). On this basis,  
223 the present work assessed whether a computational workflow could estimate the capability  
224 of ligands to elicit a kokumi perception by triggering the very early mechanism at the basis  
225 of kokumi taste, i.e. the stabilization of the closed and active structure of CaSR VFT domain.  
226 In this respect, computational methods and bioinformatics already succeeded to investigate  
227 taste peptides (Iwaniak, Minkiewicz, Darewicz, & Hryniewicz, 2016). Specifically, in this  
228 work, a 3D molecular modelling approach was used combining docking studies,  
229 pharmacophoric analysis and molecular dynamics simulations to: i) ~~understand~~ get insights  
230 on the chemical basis of VFT domain-kokumi molecule interaction; and ii) study the early  
231 molecular mechanisms of receptor activation over the time. Once assessed the model  
232 performances, a virtual library of 400  $\gamma$ -Glutamyl tripeptides was screened to identify novel  
233 and potentially strong kokumi-active sequences never described before.

### 234 **3.1. Assessment of model performances**

235 Model performances were assessed following a multi-tier approach in agreement with  
236 previous studies (e.g., (Louisse et al., 2022)). First, the capability to reproduce the binding  
237 architecture of L-Trp, taken as a kokumi reference ligand (Laffitte et al., 2021), was done

238 comparing its calculated pose with the crystallographic architecture of binding reported in  
239 the PDB structure having code 7DTU (Ling et al., 2021). As shown in Figure 1, docking  
240 simulation was able to reliably reproduce the binding architecture of L-Trp and its network  
241 of polar interactions, with an average RMSD value of 0.6 Å, confirming the geometrical  
242 reliability of the model. Then, the capability of model to discriminate between CaSR ligands  
243 (i.e., kokumi molecules) and non-ligands (i.e., kokumi-inactive molecules) was assessed  
244 combining data from docking studies and molecular dynamic simulations. Specifically, the  
245 weak CaSR activator Gly (chosen as negative controls due to its negligible kokumi activity),  
246 the moderate CaSR activator and kokumi-active molecules L-Trp, the strong activator and  
247 kokumi-active molecule  $\gamma$ -Glu-Val-Gly and the inactive  $\gamma$ -Glu-Val-Trp (chosen as a negative  
248 control) were considered in this study (Conigrave, Quinn, & Brown, 2000; Geng et al., 2016;  
249 Ohsu et al., 2010; Zhao et al., 2016). As shown in Table 1, the whole set of molecules  
250 included in this study recorded relatively high docking scores pointing to their possible  
251 capability to match pocket requirements (the higher the score, the higher the theoretical  
252 capability of ligands to match the pocket). Conversely, the inspection of docking poses  
253 revealed a substantial difference between the weak-to-strong activators (Gly, L-Trp and  $\gamma$ -  
254 Glu-Val-Gly) and the inactive sequence  $\gamma$ -Glu-Val-Trp. Specifically, the formers showed an  
255 architecture of binding that resembled the crystallographic pose of L-Trp with the alpha  
256 carboxy- and amino-group of  $\gamma$ -Glutamyl residue involved in polar contact with Ser147,  
257 Ala168 and Ser170 (Figure 2). The comparison between the docking poses and the  
258 pharmacophoric analysis of the binding pocket provided a mechanistic rationale for the  
259 experimental data reported so far for this set of molecules. In particular, the higher  
260 capability of L-Trp to activate CaSR compared to Gly could be explained, at least in part, by  
261 the better capability of the former to interact with the VFT domain. Indeed, the indole ring

262 of L-Trp was arranged within a hydrophobic region of the binding site likely adding  
263 additional hydrophobic/hydrophobic favourable interactions compared to Gly. In this  
264 respect, Gly recorded a docking score significantly lower than the other molecules, in  
265 agreement with its very weak capability to activate CaSR. These additional contributions to  
266 the binding event of L-Trp could suggest a major effect to stabilize the closed conformation  
267 of VTF domain compared to Gly determining a more effective CaSR activation and a more  
268 pronounced kokumi perception, in agreement with previous studies (Mun et al., 2004;  
269 Goralsky and Ram, 2022). Following this line of interpretation, the stronger activity of  $\gamma$ -Glu-  
270 Val-Gly could be explained by the additional contribution to the binding event due to the  
271 polar contact between its Gly C-terminus and the side chain of Asn102 (Figure 2C).  
272 Conversely,  $\gamma$ -Glu-Val-Trp, which was described as unable to activate CaSR (Ohsu et al.,  
273 2010), showed a substantially different architecture of binding which missed all the key  
274 contacts described above and reported in crystallographic studies despite the high score  
275 recorded. The incapability to mimic the binding pose of  $\gamma$ -Glu-Val-Gly was due to the local  
276 lack of a sufficient space to receive the bulky side chain of Trp at the 3<sup>rd</sup> (C-terminal)  
277 position that forced this peptide to find an alternative arrangement into the pocket. The  
278 relatively high score was reasonably due to the high number of hydrophobic/hydrophobic  
279 contributions. However, an appreciable interaction with VFT domain was not deemed likely  
280 based on the lack of the network of key polar contacts well reported by crystallographic  
281 records and calculated for  $\gamma$ -Glu-Val-Gly. In addition,  $\gamma$ -Glu-Val-Trp recorded more variable  
282 scores compared to the other ligands considered here, with a coefficient of variation (CV) of  
283 3.6 % while the other activators showed CV values below 1%. The higher variability of  $\gamma$ -Glu-  
284 Val-Trp scores could indicate the incapability to find a unique and stable binding  
285 architecture, which is typically associated with nonoptimal ligands that are unable to

286 satisfyingly match pocket requirements (Aichinger et al., 2020). Taken together these results  
287 pointed to the possible relevance and usability of docking scores and poses to distinguish  
288 CaSR activators from inactive molecules.

289 Keeping in mind that the stabilization of the closed conformation of VFT domain is a key  
290 mechanistic event underpinning CaSR activation and kokumi taste perception, the stability  
291 of VFT domain in complex with Gly, L-Trp,  $\gamma$ -Glu-Val-Gly and  $\gamma$ -Glu-Val-Trp or in the unbound  
292 state was monitored over the time with molecular dynamic simulations. In particular, the  
293 protein's  $\alpha$ -carbon root mean squared deviation (RMSD) was measured along with specific  
294 inter-molecular movements to describe VFT opening/closure (Figure 3). Specifically, three  
295 inter-atomic distances were considered to monitor VFT domain's motions and to describe  
296 either the stable maintenance of a closed conformation or its opening preluding to ligand  
297 detachment and receptor inactivation (Figure 3). -With respect to the RMSD analysis, the  
298 complexes considered and the VFT domain in the unbound state showed a similar trend  
299 similar, although the complex with  $\gamma$ -Glu-Val-Trp showed slightly higher values from 15  
300 nanoseconds onward (Figure 1S; Supporting material). This might point to a slight less stable  
301 geometrical organization of the complex with  $\gamma$ -Glu-Val-Trp compared to the other ligands  
302 or to the unbound VFT domain. Concerning the intra-molecular distances considered to  
303 monitor VFT domain closure/opening, a clearly different trend was observed for moderate  
304 and strong activators (i.e., L-Trp and  $\gamma$ -Glu-Val-Gly) compared to the weak activator Gly, the  
305 inactive peptide  $\gamma$ -Glu-Val-Trp and the unbound VFT domain. As shown in Figure 3B, the  
306 strong activator  $\gamma$ -Glu-Val-Gly and the moderate activator L-Trp showed a similar trend in  
307 the three intra-molecular contact regions (C1, C2 and C3) considered, which were kept  
308 tightly close along the whole simulation. Conversely, an early detachment was observed for  
309 all the contact regions in the unbound VFT domain (more marked for C2 than C1 or C3)

310 pointing as unfavourable the closed geometry of VFT domain in the unbound state, in  
311 agreement with previous studies (Ling et al., 2021). Of note, monitoring such intra-  
312 molecular distances could provide a semi-quantitative comparison of ligands in terms of  
313 activity: the very weak activator Gly showed for the three contact point regions considered  
314 a trend that was intermediate between the inactive sequence  $\gamma$ -Glu-Val-Trp and the two  
315 activators L-Trp and  $\gamma$ -Glu-Val-Gly. This was particularly evident for C2 and C3 where the  
316 interatomic distances tended to resemble the scenario drawn for the unbound VFT domain.  
317 In other words, Gly showed a limited capability to stabilize the closed conformation of VFT  
318 domain causing its opening as time went by during the simulation. This outcome could  
319 provide a mechanistic basis to better understand the rationale for the very weak activity  
320 reported for Gly. Concerning the inactive peptide  $\gamma$ -Glu-Val-Trp, all the interatomic distances  
321 considered constantly increased during the simulation pointing to a clear opening of the VFT  
322 domain. The close inspection of complex trajectories confirmed such hypothesis as constant  
323 opening movements were observed for all the contact regions considered (Figure 3C). As  
324 described above for Gly, this evidence provided a mechanistic rationale to understand the  
325 molecular basis underpinning the incapability of  $\gamma$ -Glu-Val-Trp to activate CaSR.  
326 Taken together, these results highlighted the usability of the 3D modelling presented to  
327 investigate the early molecular event of kokumi perception and described a combination of  
328 docking simulations, pharmacophoric analysis and molecular dynamics as a meaningful tool  
329 to estimate the CaSR-activating potential of  $\gamma$ -Glutamyl tripeptides. At the same time,  
330 although the moderate activator L-Trp was not distinguished from the stronger  $\gamma$ -Glu-Val-  
331 Gly peptide preventing the possibility to directly correlate computational results to  
332 experimental values (e.g.  $EC_{50}$ ), the reliability to semi-quantitatively estimate the CaSR-  
333 activating potential of  $\gamma$ -Glutamyl peptides was pointed out. Specifically, the procedure

334 proved efficacy to soundly distinguish moderate-to-strong  $\gamma$ -Glutamyl peptides from weak  
335 or inactive molecules.

### 336 **3.2. Virtual screening of $\gamma$ -Glutamyl peptides library**

337 Based on the reliability of modelling framework discussed above, a virtual library grouping  
338 400  $\gamma$ -Glutamyl tripeptides was screened to identify novel sequences with a high theoretical  
339 potential as CaSR activators to study in further dedicated investigations. To this end, a  
340 ligand-based virtual screening was done to pre-filter the library and identify few promising  
341 candidates to investigate with docking simulations and molecular dynamics. Such pre-  
342 screening was done using a ligand-based fast search with LiSiCA algorithm and using  $\gamma$ -Glu-  
343 Val-Gly as reference template. LiSiCA scores ideally range from 0 (no similarity found) to 1  
344 (high similarity found) and sorted  $\gamma$ -Glutamyl tripeptides according to their chemical  
345 similarity to  $\gamma$ -Glu-Val-Gly, which is one of the most potent CaSR activator and kokumi-active  
346 molecule described so far. The rationale of this choice was that chemical similarities may  
347 ensure a certain degree of conservation in terms of biological activity (CaSR-activating and  
348 kokumi properties in this case), as previously demonstrated (Lammi et al., 2021). The virtual  
349 screening results for the entire library of 400  $\gamma$ -Glu-peptides are reported in Table 1S,  
350 Supporting material. Of note, 90% of the most potent  $\gamma$ -Glutamyl peptides described by  
351 Osho and co-workers (Osho et al., 2010) (i.e., with a reported CaSR activity  $< 30 \mu\text{M}$ ) were at  
352 the top of LiSiCA rank with scores above 0.8 (Table 1S; Supporting material). This evidence  
353 validated the use of  $\gamma$ -Glu-Val-Gly as a template to search potent CaSR-activating  $\gamma$ -Glutamyl  
354 tripeptides and to enrich the top region of LiSiCA hierarchization with highly potent  
355 sequences.

356 Then, a selection of top-ranked sequences was considered for further analysis with docking  
357 studies and molecular dynamics. Among the uncharacterized sequences in terms of CaSR  
358 activity at the time of analysis and to the best of our knowledge,  $\gamma$ -Glu-Pro-Ala,  $\gamma$ -Glu-Ile-Ala,  
359  $\gamma$ -Glu-Pro-Ser,  $\gamma$ -Glu-Ile-Cys and  $\gamma$ -Glu-Ile-Pro were chosen based on their sequence  
360 analogies to highly potent sequences already described (Table 1S; Supporting material) to  
361 maximize the chance to identify novel potent CaSR-activating  $\gamma$ -Glutamyl tripeptides. As  
362 shown in Figure 2, and despite the relatively high and stable scores recorded (Table 1),  $\gamma$ -  
363 Glu-Ile-Cys and  $\gamma$ -Glu-Ile-Pro showed a pose similar to the inactive peptide  $\gamma$ -Glu-Val-Trp.  
364 Therefore, their pose was considered not promising to stabilize a closed conformation of  
365 VFT domain and were not considered for further analysis. Conversely,  $\gamma$ -Glu-Pro-Ala,  $\gamma$ -Glu-  
366 Ile-Ala and  $\gamma$ -Glu-Pro-Ser showed a binding pose similar to  $\gamma$ -Glu-Val-Gly and drawn a  
367 comparable network of polar interactions with the pocket suggesting that they could  
368 efficiently stabilize the closed conformation of VFT domain. This hypothesis was further  
369 assessed with molecular dynamic simulations. As shown in Figure 3D,  $\gamma$ -Glu-Ile-Ala caused  
370 an opening of the VFT domain as suggested by the increase of interatomic distances at the  
371 contact regions C1, C2 and C3. On this basis, it was not deemed to be a potent CaSR-  
372 activating peptide. Conversely, the interaction of  $\gamma$ -Glu-Pro-Ala and  $\gamma$ -Glu-Pro-Ser  
373 determined the stable closure of the receptor over the time, and they were both considered  
374 theoretically potent CaSR-activating and kokumi-tasting  $\gamma$ -Glutamyl peptides worthy of  
375 further dedicated analysis. Of note,  $\gamma$ -Glu-Pro-Ala showed a closure tighter than both  $\gamma$ -Glu-  
376 Pro-Ser and  $\gamma$ -Glu-Val-Gly at the contact region C3 possibly pointing to a marked capability  
377 to stabilize the closed conformation of VTF domain with possible consequences on its  
378 kokumi perception.

379 From a general point of view, the lack of appreciable activity calculated for  $\gamma$ -Glu-Ile-Ala,  $\gamma$ -  
380 Glu-Ile-Cys and  $\gamma$ -Glu-Ile-Pro agreed with the data available so far in terms of potent CaSR-  
381 activating  $\gamma$ -Glutamyl tripeptides. Indeed, among the most potent sequences reported so  
382 far, the 2<sup>nd</sup> position of  $\gamma$ -Glutamyl tripeptides is rarely occupied by bulky residues and Ile is  
383 reported at the 2<sup>nd</sup> position in the reference set of already characterized  $\gamma$ -Glutamyl  
384 tripeptides (Table 1S; Supporting material) only in one moderately active sequence ( $\gamma$ -Glu-  
385 Ile-Gly). This evidence is in line with the observed limited space the pocket had to receive  
386 the side chain of residues at the 2<sup>nd</sup> position (Figure 4A). This structural requirement was  
387 reasonably at the basis of the VFT domain opening to allow the arrangement of the bulky  
388 side chain at the 2<sup>nd</sup> position of  $\gamma$ -Glu-Ile-Ala and might generally determine either a low or  
389 no activation of CaSR by  $\gamma$ -Glutamyl tripeptide with bulky side chains at the 2<sup>nd</sup> position.  
390 Conversely, less bulky side chains, like Val, ~~or~~ Pro or Cys, could be better tolerated at the 2<sup>nd</sup>  
391 position, and they may efficiently stabilize the closed and active conformation of VFT  
392 domain, in line with the evidence reported for the reference set of  $\gamma$ -Glutamyl tripeptides  
393 (Table 1S; Supporting material). Specifically, although the pharmacophoric analysis revealed  
394 regions able to receive polar groups (Figure 3S; Supporting material), steric constraints at  
395 the 2<sup>nd</sup> position seemed important to determine the capability of  $\gamma$ -Glutamyl tripeptide to  
396 properly bind the VFT, in line with the lack of potent kokumi  $\gamma$ -Glutamyl tripeptide with a  
397 bulky polar residue at the 2<sup>nd</sup> position (Table 1S; Supporting material). In this respect, the  
398 reference set of  $\gamma$ -Glutamyl tripeptides (Table 1S; Supporting material) included only one  
399 kokumi active peptide with a polar (and small) residue at the 2<sup>nd</sup> position, i.e.  $\gamma$ -Glutamyl-  
400 Thr-Gly, further supporting this hypothesis. Concerning the space receiving the side chains  
401 in 3<sup>rd</sup> position (C-terminus), the analysis of VFT domain binding site revealed an opening to a  
402 solvent exposed region (Figure 4B) that could explain the higher tolerance for bulky side

403 chains as observed for some CaSR-activating  $\gamma$ -Glutamyl tripeptides (e.g.,  $\gamma$ -Glu-Val-Phe and  
404  $\gamma$ -Glu-Val-Arg, Table 1S; Supporting material). Nonetheless, the existence of a certain  
405 specificity could be inferred considering the incapability of  $\gamma$ -Glu-Val-Trp to properly dock  
406 the binding site and to activate CaSR.

407

#### 408 **4. Conclusion**

409 The identification of kokumi molecules, although still challenging, is important to  
410 understand the chemistry of food and related consequences on diet habits and consumer  
411 behaviour. The recent advances in the comprehension of mechanisms underpinning kokumi  
412 perception, and in particular the identification of CaSR as the receptor responsible for  
413 kokumi molecules recognition, paved the way to use molecular modelling approaches as a  
414 meaningful tool of analysis. In this context, the present work showed that modelling the  
415 interaction with the CaSR's VFT domain could efficiently estimate the activating potential of  
416  $\gamma$ -Glutamyl tripeptides. In particular, the study identified relevant early mechanistic features  
417 at the basis of CaSR activation, such as the way  $\gamma$ -Glutamyl tripeptides arranged into the  
418 binding site and the related effects on VFT domain opening, that could be efficiently  
419 modelled to ~~extend knowledge on~~ understand the chemistry of  $\gamma$ -Glutamyl tripeptides and  
420 used to estimate the potential of still uncharacterized sequences. This may be used in future  
421 bulk analysis for a systematic and high throughput analysis supporting the characterization  
422 of taste molecules in food. In addition, this study described precisely structural features  
423 affecting CaSR-activating potential of  $\gamma$ -Glutamyl tripeptides and the 3D structure-activity  
424 relationship analysis could serve as a useful blueprint to improve the understanding of  
425 chemical basis for kokumi molecules. Also assessing the interaction between the  $\gamma$ -Glutamyl

426 tripeptide under analysis and other GPCRs might be considered for further analysis to better  
427 characterize the biological activity beyond their taste properties, in line with the various  
428 activity they may exert in living organisms (Lu et al., 2021).

429 Overall, this work provided a useful, reliable and high-throughput tool for a top-down  
430 screening of  $\gamma$ -Glutamyl tripeptides which may be integrated into the conventional  
431 characterization and sensory tests of taste molecules facilitating the fingerprinting of  
432 kokumi compounds in food. Similarly, the model could help the rational design of libraries of  
433 compounds in the context of the *de novo* synthesis of kokumi molecules.

434 Finally, two molecules with a high potential in terms of CaSR activating properties and  
435 kokumi taste were identified (i.e.,  $\gamma$ -Glu-Pro-Ala and  $\gamma$ -Glu-Pro-Ser). Although such  
436 molecules have been prioritized for further dedicated investigations and sensory tests to  
437 ultimately verify their actual kokumi properties, it is advised their inclusion in the list of  
438 molecules to check in food matrices to characterize their possible kokumi fingerprint at a  
439 molecular level.

440

#### 441 **Declaration of interest**

442 The authors have nothing to disclose.

443

#### 444 **Acknowledgment**

445 This research benefits from the HPC (high performance computing) facility of the University  
446 of Parma, Italy.

447

448 **References**

- 449 Abraham, M. J., Murtola, T., Schulz, R., Páll, S., Smith, J. C., Hess, B., & Lindahl, E. (2015). GROMACS:  
450 High performance molecular simulations through multi-level parallelism from laptops to  
451 supercomputers. *SoftwareX*, 1-2, 19-25.
- 452 Aichinger, G., Dellafiora, L., Pantazi, F., Del Favero, G., Galaverna, G., Dall'Asta, C., & Marko, D.  
453 (2020). Alternaria toxins as casein kinase 2 inhibitors and possible consequences for  
454 estrogenicity: a hybrid in silico/in vitro study. *Archives of Toxicology*, 94 (6), 2225-2237.
- 455 Best, R. B., Zhu, X., Shim, J., Lopes, P. E. M., Mittal, J., Feig, M., & MacKerell, A. D. (2012).  
456 Optimization of the Additive CHARMM All-Atom Protein Force Field Targeting Improved  
457 Sampling of the Backbone phi, psi and Side-Chain chi(1) and chi(2) Dihedral Angles. *Journal*  
458 *of Chemical Theory and Computation*, 8 (9), 3257-3273.
- 459 Bo, W., Qin, D., Zheng, X., Wang, Y., Ding, B., Li, Y., & Liang, G. (2022). Prediction of bitterant and  
460 sweetener using structure-taste relationship models based on an artificial neural network.  
461 *Food Research International*, 153, 110974.
- 462 Chartier, M., & Najmanovich, R. (2015). Detection of Binding Site Molecular Interaction Field  
463 Similarities. *Journal of Chemical Information and Modeling*, 55 (8), 1600-1615.
- 464 Conigrave, A. D., Quinn, S. J., & Brown, E. M. (2000). L-Amino acid sensing by the extracellular Ca<sup>2+</sup>-  
465 sensing receptor. *Proceedings of the National Academy of Sciences of the United States of*  
466 *America*, 97 (9), 4814-4819.
- 467 Dellafiora, L., Ruotolo, R., Perotti, A., Cirilini, M., Galaverna, G., Cozzini, P., Buschini, A., & Dall'Asta, C.  
468 (2017). Molecular insights on xenoestrogenic potential of zearalenone-14-glucoside through  
469 a mixed in vitro/in silico approach. *Food and Chemical Toxicology*, 108, 257-266.
- 470 Gaudreault, F., Morency, L. P., & Najmanovich, R. J. (2015). NRGsuite: a PyMOL plugin to perform  
471 docking simulations in real time using FlexAID. *Bioinformatics*, 31 (23), 3856-3858.
- 472 Geng, Y., Mosyak, L., Kurinov, I., Zuo, H., Sturchler, E., Cheng, T. C., Subramanyam, P., Brown, A. P.,  
473 Brennan, S. C., Mun, H. C., Bush, M., Chen, Y., Nguyen, T. X., Cao, B. H., Chang, D. D., Quick,

474 M., Conigrave, A. D., Colecraft, H. M., McDonald, P., & Fan, Q. R. (2016). Structural  
475 mechanism of ligand activation in human calcium-sensing receptor. *Elife*, 5.

476 Goralski, T., & Ram, J. L. (2022). Extracellular Calcium Receptor as a Target for Glutathione and Its  
477 Derivatives. *International Journal of Molecular Sciences*, 23 (2).

478 Guha, S., & Majumder, K. (2022). Comprehensive Review of  $\gamma$ -Glutamyl Peptides ( $\gamma$ -GPs) and Their  
479 Effect on Inflammation Concerning Cardiovascular Health. *Journal of Agricultural and Food*  
480 *Chemistry*.

481 Huang, L., Zhao, Y. J., Dong, Q. R., & Hu, G. C. (2021). A study of altered calcium sensing system  
482 caused primary membranous nephropathy to end-stage renal failure. *Biomedicine &*  
483 *Pharmacotherapy*, 141.

484 Iwaniak, A., Minkiewicz, P., Darewicz, M., & Hryniewicz, M. (2016). Food protein-originating  
485 peptides as tastants - Physiological, technological, sensory, and bioinformatic approaches.  
486 *Food Research International*, 89, 27-38.

487 Keast, R., Costanzo, A., & Hartley, I. (2021). Macronutrient Sensing in the Oral Cavity and  
488 Gastrointestinal Tract: Alimentary Tastes. *Nutrients*, 13 (2).

489 Kim, J., Ahmad, R., Deb-Choudhury, S., Subbaraj, A., Dalziel, J. E., & Knowles, S. O. (2022). Generation  
490 and identification of kokumi compounds and their validation by taste-receptor assay: An  
491 example with dry-cured lamb meat. *Food Chemistry: X*, 13, 100218.

492 Kim, S., Chen, J., Cheng, T. J., Gindulyte, A., He, J., He, S. Q., Li, Q. L., Shoemaker, B. A., Thiessen, P.  
493 A., Yu, B., Zaslavsky, L., Zhang, J., & Bolton, E. E. (2021). PubChem in 2021: new data content  
494 and improved web interfaces. *Nucleic Acids Research*, 49 (D1), D1388-D1395.

495 Kuroda, M., Kato, Y., Yamazaki, J., Kai, Y., Mizukoshi, T., Miyano, H., & Eto, Y. (2013). Determination  
496 and quantification of the kokumi peptide, gamma-glutamyl-valyl-glycine, in commercial soy  
497 sauces. *Food Chemistry*, 141 (2), 823-828.

498 Laffitte, A., Gibbs, M., de Alvaro, C. H., Addison, J., Lonsdale, Z. N., Giribaldi, M. G., Rossignoli, A.,  
499 Vennegeerts, T., Winnig, M., Klebansky, B., Skiles, J., Logan, D. W., & McGrane, S. J. (2021).

500 Kokumi taste perception is functional in a model carnivore, the domestic cat (*Felis catus*).  
501 *Scientific Reports*, 11 (1).

502 Lammi, C., Boschin, G., Bollati, C., Arnoldi, A., Galaverna, G., & Dellafiora, L. (2021). A heuristic,  
503 computer-driven and top-down approach to identify novel bioactive peptides: A proof-of-  
504 principle on angiotensin I converting enzyme inhibitory peptides. *Food Research*  
505 *International*, 150.

506 Legnik, S., Stular, T., Brus, B., Knez, D., Gobec, S., Janezic, D., & Konc, J. (2015). LiSiCA: A Software for  
507 Ligand-Based Virtual Screening and Its Application for the Discovery of Butyrylcholinesterase  
508 Inhibitors. *Journal of Chemical Information and Modeling*, 55 (8), 1521-1528.

509 Li, Q., Zhang, L. T., & Lametsch, R. (2022). Current progress in kokumi-active peptides, evaluation and  
510 preparation methods: a review. *Critical Reviews in Food Science and Nutrition*, 62 (5), 1230-  
511 1241.

512 Ling, S. L., Shi, P., Liu, S. L., Meng, X. Y., Zhou, Y. X., Sun, W. J., Chang, S. H., Zhang, X., Zhang, L. H.,  
513 Shi, C. W., Sun, D. M., Liu, L., & Tian, C. L. (2021). Structural mechanism of cooperative  
514 activation of the human calcium-sensing receptor by Ca<sup>2+</sup> ions and L-tryptophan. *Cell*  
515 *Research*, 31 (4), 383-394.

516 Lousse, J., Dorne, J. L. C. M., & Dellafiora, L. (2022). Investigating the interaction between organic  
517 anion transporter 1 and ochratoxin A: An in silico structural study to depict early molecular  
518 events of substrate recruitment and the impact of single point mutations. *Toxicology*  
519 *Letters*, 355, 19-30.

520 Lu, Y. J., Wang, J., Soladoye, O. P., Aluko, R. E., Fu, Y., & Zhang, Y. H. (2021). Preparation, receptors,  
521 bioactivity and bioavailability of gamma-glutamyl peptides: A comprehensive review. *Trends*  
522 *in Food Science & Technology*, 113, 301-314.

523 Maruyama, Y., Yasuda, R., Kuroda, M., & Eto, Y. (2012). Kokumi Substances, Enhancers of Basic  
524 Tastes, Induce Responses in Calcium-Sensing Receptor Expressing Taste Cells. *Plos One*, 7 (4).

525 Mun, H. C., Franks, A. H., Culverston, E. L., Krapcho, K., Nemeth, E. F., & Conigrave, A. D. (2004). The  
526 Venus fly trap domain of the extracellular Ca<sup>2+</sup>-sensing receptor is required for L-amino acid  
527 sensing. *Journal of Biological Chemistry*, 279 (50), 51739-51744.

528 O'Boyle, N. M., Banck, M., James, C. A., Morley, C., Vandermeersch, T., & Hutchison, G. R. (2011).  
529 Open Babel: An open chemical toolbox. *Journal of Cheminformatics*, 3.

530 Ohsu, T., Amino, Y., Nagasaki, H., Yamanaka, T., Takeshita, S., Hatanaka, T., Maruyama, Y.,  
531 Miyamura, N., & Eto, Y. (2010). Involvement of the Calcium-sensing Receptor in Human  
532 Taste Perception. *Journal of Biological Chemistry*, 285 (2), 1016-1022.

533 Ruijschop, R., Burseg, K. M. M., Lambers, T. T., & Overduin, J. (2009). Designing foods to induce  
534 satiation: a flavour perspective. In D. J. McClements & E. A. Decker (Eds.), *Designing*  
535 *Functional Foods: Measuring and Controlling Food Structure Breakdown and Nutrient*  
536 *Absorption* (pp. 623-646).

537 Schrader, M. (2018). Origins, Technological Development, and Applications of Peptidomics. In M.  
538 Schrader & L. Fricker (Eds.), *Peptidomics: Methods and Strategies* (Vol. 1719, pp. 3-39).

539 Simons, K. T., Bonneau, R., Ruczinski, I., & Baker, D. (1999). Ab initio protein structure prediction of  
540 CASP III targets using ROSETTA. *Proteins-Structure Function and Bioinformatics*, 171-176.

541 Smith, K. H., Tejada-Montes, E., Poch, M., & Mata, A. (2011). Integrating top-down and self-assembly  
542 in the fabrication of peptide and protein-based biomedical materials. *Chemical Society*  
543 *Reviews*, 40 (9), 4563-4577.

544 Spaggiari, G., Di Pizio, A., & Cozzini, P. (2020). Sweet, umami and bitter taste receptors: State of the  
545 art of in silico molecular modeling approaches. *Trends in Food Science & Technology*, 96, 21-  
546 29.

547 Sundararaman, S. S., & van der Vorst, E. P. C. (2021). Calcium-Sensing Receptor (CaSR), Its Impact on  
548 Inflammation and the Consequences on Cardiovascular Health. *International Journal of*  
549 *Molecular Sciences*, 22 (5).

550 Tang, C. S., Tan, V. W. K., Teo, P. S., & Forde, C. G. (2020). Savoury and kokumi enhancement  
551 increases perceived calories and expectations of fullness in equicaloric beef broths. *Food*  
552 *Quality and Preference*, 83.

553 Toelstede, S., Dunkel, A., & Hofmann, T. (2009). A Series of Kokumi Peptides Impart the Long-Lasting  
554 Mouthfulness of Matured Gouda Cheese. *Journal of Agricultural and Food Chemistry*, 57 (4),  
555 1440-1448.

556 Toelstede, S., & Hofmann, T. (2008). Sensomics mapping and identification of the key bitter  
557 metabolites in Gouda cheese. *Journal of Agricultural and Food Chemistry*, 56 (8), 2795-2804.

558 Vasilaki, A., Panagiotopoulou, E., Koupantsis, T., Katsanidis, E., & Mourtzinis, I. Recent insights in  
559 flavor-enhancers: Definition, mechanism of action, taste-enhancing ingredients, analytical  
560 techniques and the potential of utilization. *Critical Reviews in Food Science and Nutrition*.

561 Wellendorph, P., & Brauner-Osborne, H. (2009). Molecular basis for amino acid sensing by family C  
562 G-protein-coupled receptors. *British Journal of Pharmacology*, 156 (6), 869-884.

563 Yang, J., Huang, Y. R., Cui, C., Dong, H., Zeng, X. F., & Bai, W. D. (2021). Umami-enhancing effect of  
564 typical kokumi-active gamma-glutamyl peptides evaluated via sensory analysis and  
565 molecular modeling approaches. *Food Chemistry*, 338.

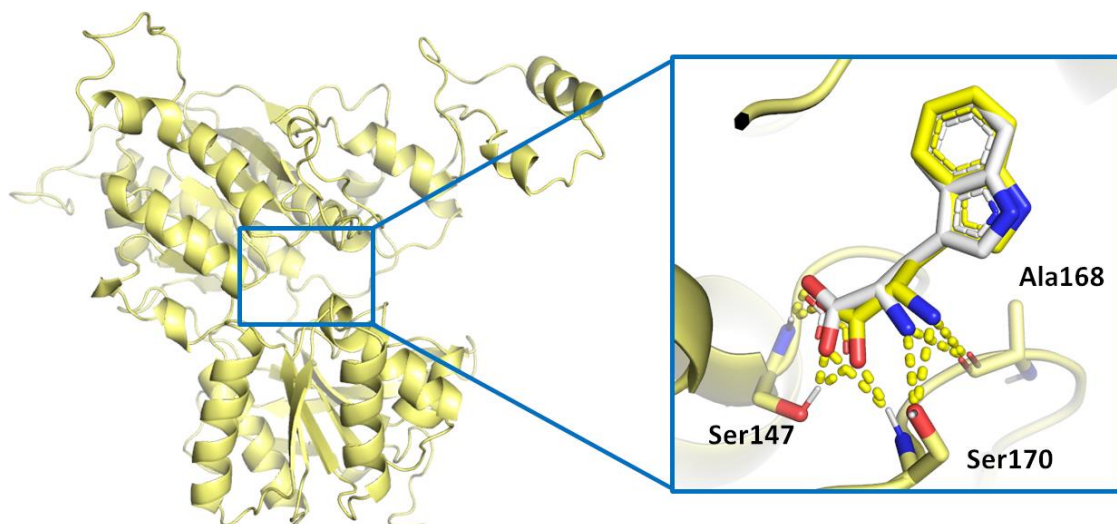
566 Yang, J. Y., Anishchenko, I., Park, H., Peng, Z. L., Ovchinnikov, S., & Baker, D. (2020). Improved  
567 protein structure prediction using predicted interresidue orientations. *Proceedings of the*  
568 *National Academy of Sciences of the United States of America*, 117 (3), 1496-1503.

569 Zhang, C., Zhang, T., Zou, J., Miller, C. L., Gorkhali, R., Yang, J. Y., Schillmiller, A., Wang, S., Huang, K.,  
570 Brown, E. M., Moremen, K. W., Hu, J., & Yang, J. J. (2016). Structural basis for regulation of  
571 human calcium-sensing receptor by magnesium ions and an unexpected tryptophan  
572 derivative co-agonist. *Science Advances*, 2 (5).

573 Zhao, C. J., Schieber, A., & Ganzle, M. G. (2016). Formation of taste-active amino acids, amino acid  
574 derivatives and peptides in food fermentations - A review. *Food Research International*, 89,  
575 39-47.

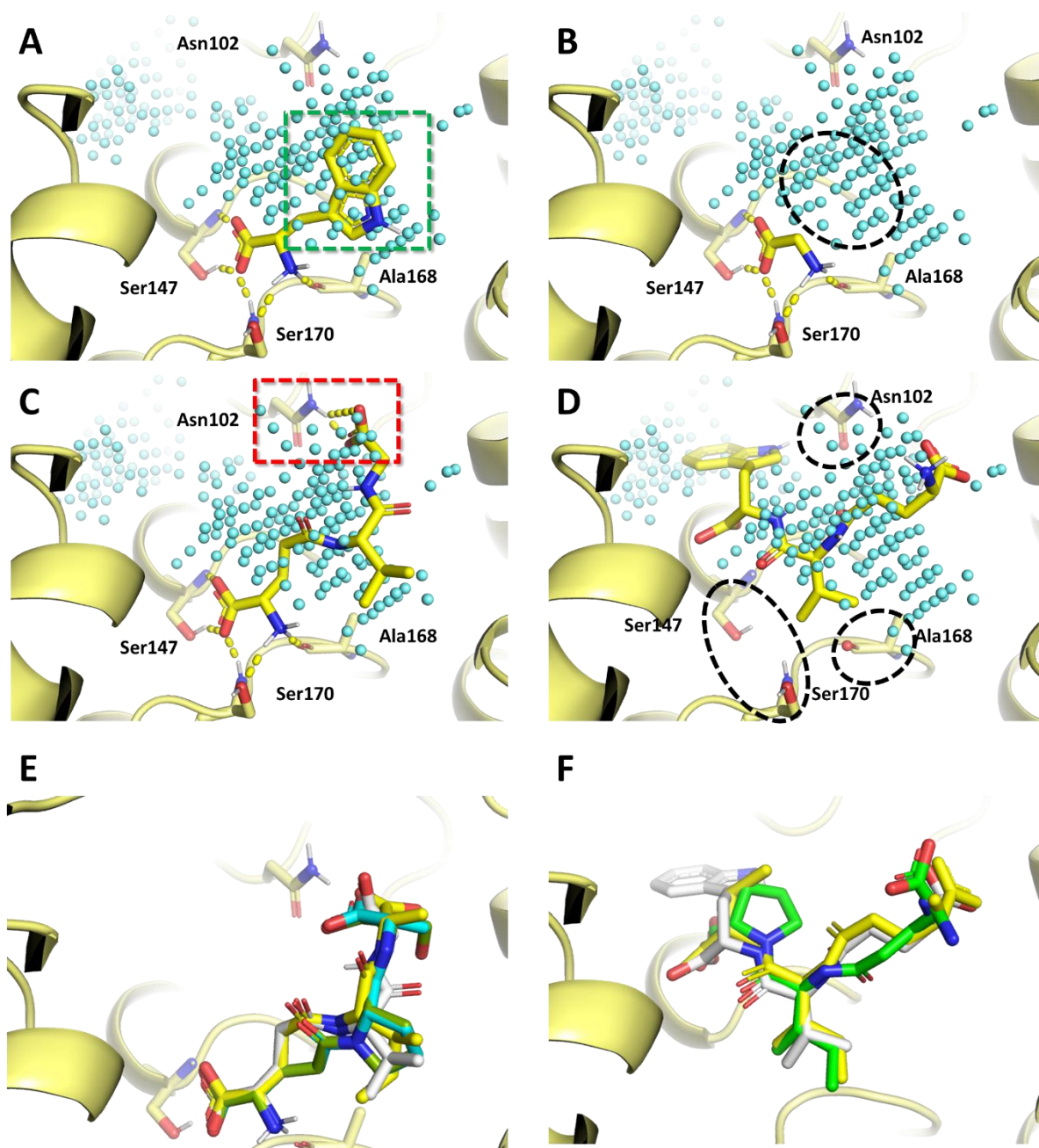
576 Zoete, V., Cuendet, M. A., Grosdidier, A., & Michielin, O. (2011). SwissParam: A Fast Force Field  
577 Generation Tool for Small Organic Molecules. *Journal of Computational Chemistry*, 32 (11),  
578 2359-2368.  
579

580 **Figures**



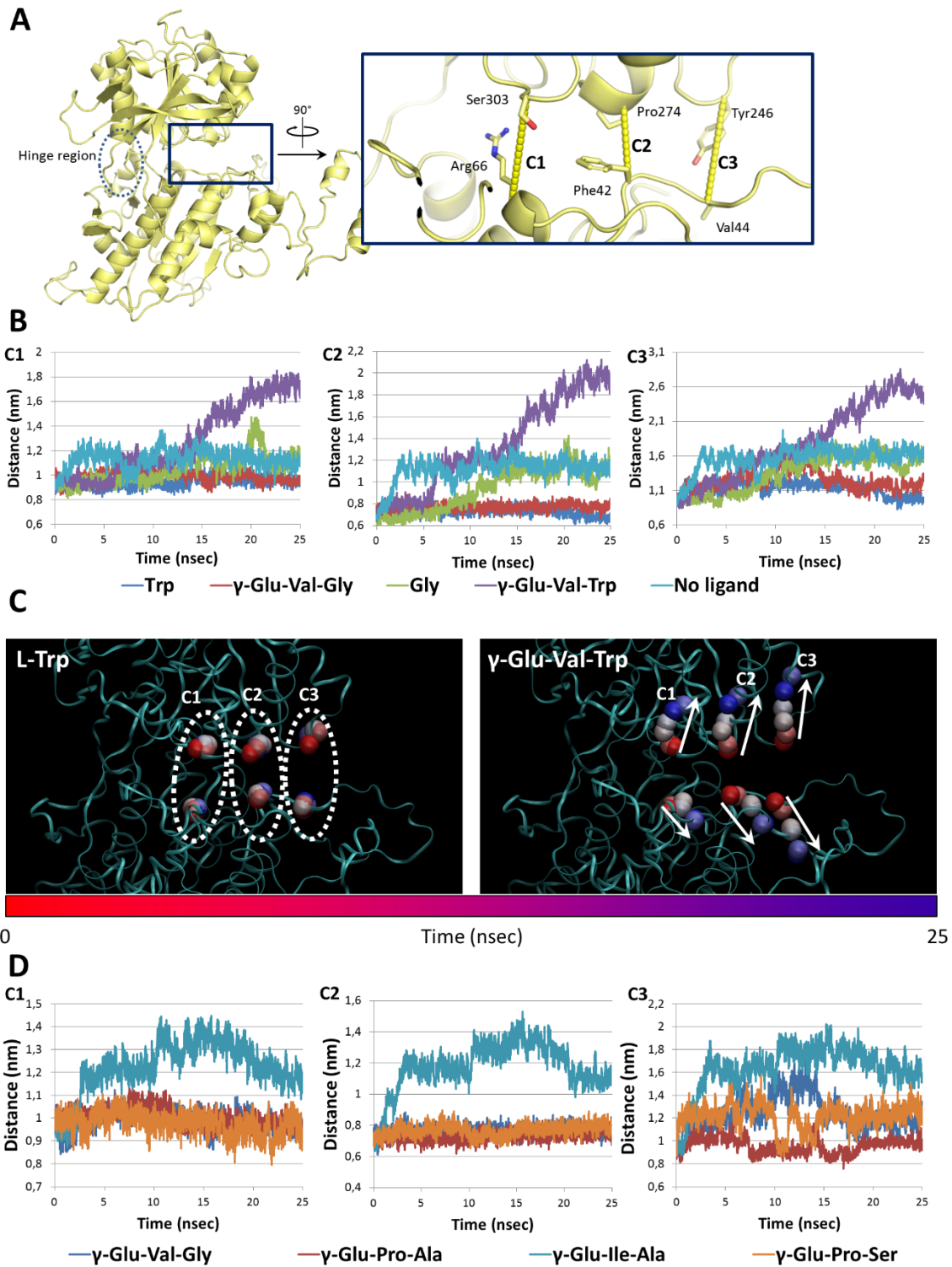
581

582 **Figure 1.** Graphical representation of CaSR VTF domain. The protein is represented in  
583 cartoon while ligands are represented in stick. The close-up on the right reports the  
584 comparison between the calculated (yellow) and crystallographic (white) pose of L-Trp.  
585 Yellow dashed lined indicate to formation of polar contacts.



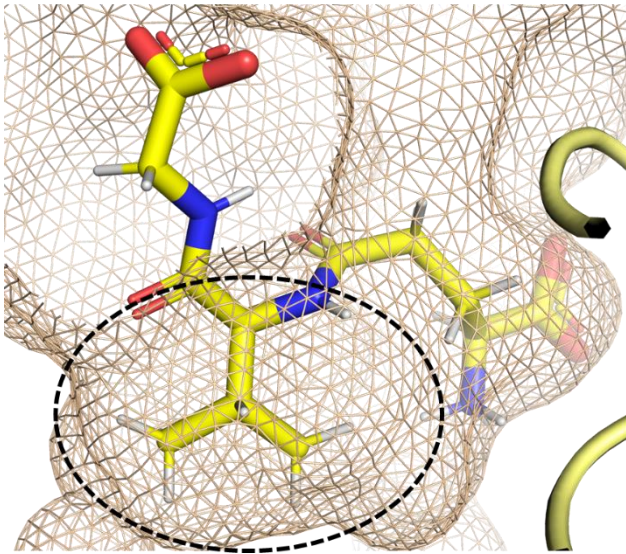
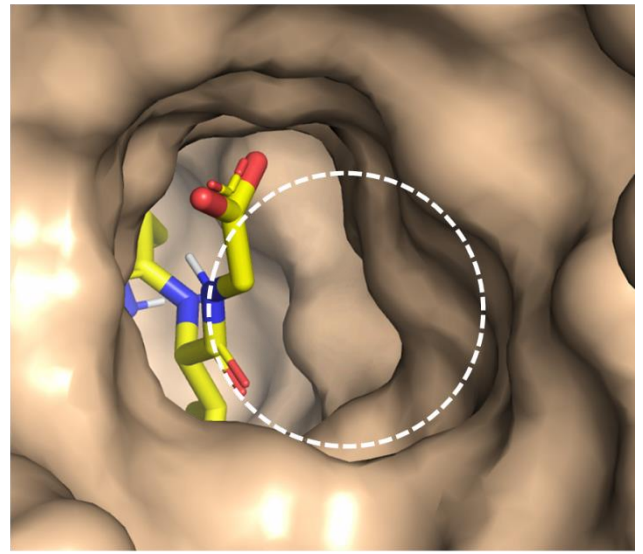
586  
587 **Figure 2.** Docking pose of molecules under investigation. The protein is represented in  
588 cartoon while ligands and protein's amino acids involved in polar contacts are represented  
589 in sticks. Yellow dashed lines indicate polar contacts while cyan spheres represent the  
590 region of the binding pocket energetically suitable to receive hydrophobic groups. **A.** L-Trp.  
591 The green dashed box indicates the proper arrangement of the hydrophobic indole ring  
592 within a region of the pocket suitable to receive hydrophobic groups. **B.** Gly. The dashed  
593 black ring indicates the lack of hydrophobic-hydrophobic interactions. **C.**  $\gamma$ -Glu-Val-Gly. The

594 red dashed box indicates the additional polar contact between the peptide C-terminus (Gly  
595 at the 3rd position) and the side chain of Asn102. **D.**  $\gamma$ -Glu-Val-Trp. The dashed black rings  
596 indicate the lack of interaction with the residues engaged by the other molecules under  
597 investigation. **E.** Docking pose superimposition of  $\gamma$ -Glu-Val-Gly (white),  $\gamma$ -Glu-Ile-Ala  
598 (yellow),  $\gamma$ -Glu-Pro-Ser (green) and  $\gamma$ -Glu-Pro-Ala (cyan). **F.** Docking pose superimposition of  
599  $\gamma$ -Glu-Val-Trp (white),  $\gamma$ -Glu-Ile-Cys (yellow) and  $\gamma$ -Glu-Ile-Pro (green).



600  
 601 **Figure 3.** Molecular dynamics results. **A.** Graphical representation of CaSR in cartoon. The  
 602 dashed ring indicates the hinge region while the three intra-molecular contact region  
 603 distances considered to measure the opening of VFT domain are indicated with yellow  
 604 dashed lines in the close-up on the right. Specifically, three contact regions (C1, C2 and C3)  
 605 were defined between the  $\alpha$ -carbon of Arg66-Ser303, Pro274-Phe42 and Tyr246-Val44,

606 respectively. **B.** Distance plots of C1, C2 and C3 contact regions for VTF domain in complex  
607 with Gly, L-Trp,  $\gamma$ -Glu-Val-Gly,  $\gamma$ -Glu-Val-Trp or in the unbound state. **C.** Trajectory analysis of  
608 contact region C1, C2 and C3 for VTF domain in complex with L-Trp or  $\gamma$ -Glu-Val-Trp. The  
609 from-red-to-blue colour switch indicates the stepwise changes of coordinates during the  
610 simulation. The dashed white rings indicate the stable fluctuation of interatomic distances  
611 for C1, C2 and C3 contact regions when VTF domain was in complex with L-Trp. Conversely,  
612 white arrows indicate the progressive detachment of C1, C2 and C3 contact regions for VTF  
613 domain in complex with  $\gamma$ -Glu-Val-Trp leading to the structure opening. **D.** Distance plots of  
614 C1, C2 and C3 contact regions for VTF domain in complex with  $\gamma$ -Glu-Val-Gly (taken as  
615 reference),  $\gamma$ -Glu-Pro-Ala,  $\gamma$ -Glu-Ile-Ala or  $\gamma$ -Glu-Pro-Ser.

**A****B**

616

617

**Figure 4.** Close-ups of the pocket environment surrounding  $\gamma$ -Glu-Val-Gly. **A.** Focus on the

618 space surrounding the side chain of Val at the 2<sup>nd</sup> position. The pocket is represented in

619 mesh while  $\gamma$ -Glu-Val-Gly is represented in sticks. The black dashed ring indicates the almost

620 full sub-site occupancy by Val side chain. **B.** Focus on the space surrounding Gly at the 3<sup>rd</sup>

621 position. The pocket is represented in solid surface while  $\gamma$ -Glu-Val-Gly is represented in

622 sticks. The white dashed ring indicates the presence of a solvent exposed region of the VTF

623 domain binding site that could be occupied by the side chain of certain amino acids at the

624 3<sup>rd</sup> position of  $\gamma$ -Glutamyl tripeptides.

**Table 1.** Docking scores and reported activity of molecules under analysis

<b>Peptide</b>	<b>Docking score (mean <math>\pm</math> SD)<sup>1</sup></b>	<b>Experimental activity</b>
Gly	58.65 $\pm$ 0.04	Very weak activator <sup>2</sup>
L-Trp	103.37 $\pm$ 0.16	Moderate activator <sup>3</sup>
$\gamma$ -Glu-Val-Gly	116.70 $\pm$ 0.90	Strong activator <sup>4</sup>
$\gamma$ -Glu-Val-Trp	115.65 $\pm$ 4.14	Inactive <sup>4</sup>
$\gamma$ -Glu-Pro-Ala	123.26 $\pm$ 0.86	Unknown
$\gamma$ -Glu-Ile-Ala	121.86 $\pm$ 0.36	Unknown
$\gamma$ -Glu-Pro-Ser	125.54 $\pm$ 1.16	Unknown
$\gamma$ -Glu-Ile-Cys	124.41 $\pm$ 0.82	Unknown
$\gamma$ -Glu-Ile-Pro	115.42 $\pm$ 0.39	Unknown

*Note:* <sup>1</sup> Docking scores are expressed as mean  $\pm$  SD of three replicates. <sup>2</sup> According to (Geng et al., 2016). <sup>3</sup> According to (Conigrave et al., 2000). <sup>4</sup> According to (Ohsu et al., 2010).



[Click here to access/download](#)

**Supplementary material for online publication only**  
**R2\_SM\_Gustav\_FRI.docx**

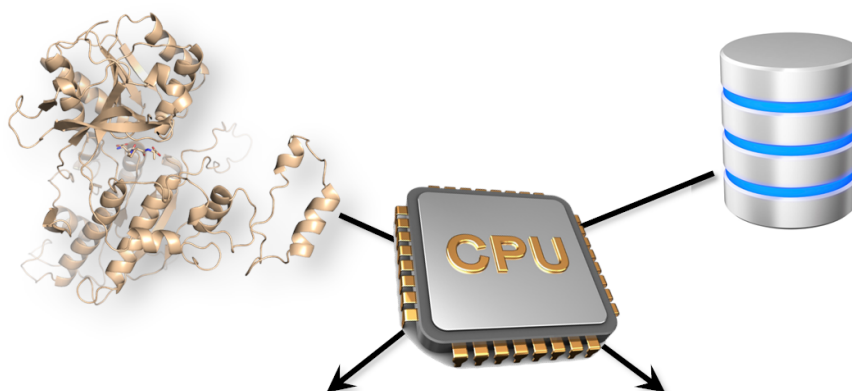


Graphical abstract

# A mechanistic investigation on kokumi-active $\gamma$ -Glutamyl tripeptides

3D model of CaSR's venus flytrap domain

Virtual library of 400  $\gamma$ -Glutamyl tripeptides



3D structure-activity relationship analysis of kokumi-active  $\gamma$ -Glutamyl tripeptides

Tool for the top-down identification of kokumi-active molecules

**CRedit author statement**

**Luca Dellafiora:** Conceptualization, Methodology, Software, Formal analysis, Investigation, Writing - Original Draft, Writing - Review & Editing, Supervision

**Fabio Magnaghi:** Methodology, Software, Formal analysis, Investigation, Writing - Original Draft

**Gianni Galaverna:** Conceptualization, Writing - Original Draft, Writing - Review & Editing

**Chiara Dall'Asta:** Conceptualization, Writing - Original Draft, Writing - Review & Editing, Supervision